Letter

Localized Enzymatic Degradation of Polymers: Physics and Scaling Laws

Shankar Lalitha Sridhar and Franck Vernerey*

Department of Mechanical Engineering, University of Colorado Boulder, Boulder, Colorado 80309, USA

(Received 15 October 2017; published 16 March 2018)

Biodegradable polymers are naturally abundant in living matter and have led to great advances in controlling environmental pollution due to synthetic polymer products, harnessing renewable energy from biofuels, and in the field of biomedicine. One of the most prevalent mechanisms of biodegradation involves enzyme-catalyzed depolymerization by biological agents. Despite numerous studies dedicated to understanding polymer biodegradation in different environments, a simple model that predicts the macroscopic behavior (mass and structural loss) in terms of microphysical processes (enzyme transport and reaction) is lacking. An interesting phenomenon occurs when an enzyme source (released by a biological agent) attacks a tight polymer mesh that restricts free diffusion. A fuzzy interface separating the intact and fully degraded polymer propagates away from the source and into the polymer as the enzymes diffuse and react in time. Understanding the characteristics of this interface will provide crucial insight into the biodegradation process and potential ways to precisely control it. In this work, we present a centrosymmetric model of biodegradation by characterizing the moving fuzzy interface in terms of its speed and width. The model predicts that the characteristics of this interface are governed by two time scales, namely the polymer degradation and enzyme transport times, which in turn depend on four main polymer and enzyme properties. A key finding of this work is simple scaling laws that can be used to guide biodegradation of polymers in different applications.

DOI: 10.1103/PhysRevApplied.9.031001

I. INTRODUCTION

Biodegradation of polymers is the process of breakdown of the polymeric network by biological agents into components that naturally blend into the environment. The biological agents can be macro-organisms that digest the polymer through mechanical and chemical processes or micro-organisms that degrade and consume the polymer by secreting enzymes or other byproducts like acids [1,2]. Enzymes are biological catalysts that have the ability to cleave polymer chains. For instance, fungi have been found to break down natural polymer networks such as wood and tissues [3]. A notable example is the wood-decay fungus that has the special ability to break down lignin, cellulose, and hemicellulose, three inert but essential polymers in the plant cell wall [4]. Detailed studies of the degradation process initiated by these fungi have led to great progress in the bioenergy industry in breaking down biomass, the largest source of renewable energy, using enzyme technology [5]. Digestive processes in most organisms are mediated by digestive enzymes that degrade natural polymers like protein, abundantly found in food sources [6]. Perhaps the most widely understood meaning of biodegradation is in relation to synthetic polymers or plastics that raise serious environmental concerns. Many advances have been made in altering the chemical composition of synthetic polymers to make them more suitable for biodegradation in the natural environment [7]. Biodegradable polymers have also found their way into biomedicine through implantable biomedical devices [8,9], hydrogel scaffolds for tissue regrowth [10–12], and polymeric drug delivery vehicles [13–15].

Polymer degradation is generally measured macroscopically in terms of the overall loss in polymer mass with time for different environmental conditions. At the microscopic scale, however, multiple physical processes occur simultaneously. The mechanism of enzymatic biodegradation broadly includes enzyme diffusion from a biological source and an enzyme-catalyzed reaction (aerobic or anaerobic) that causes depolymerization. Because of restricted enzyme diffusion through the polymer mesh, an interface between the depolymerized fluid and the intact solid polymer is formed and set in motion as the enzymatic reaction proceeds. This type of a moving interface phenomenon has been widely observed with surface erosion behavior in biodegradable polymers due to water diffusion and progressive hydrolysis [16]. To better understand the factors that influence the evolution of polymer degradation, it is important to develop simple models and scaling laws based on multiple physical processes that bridge microphysical and macrophysical behavior. The focus of this work, therefore, is on developing a centrosymmetric model of polymer biodegradation by enzymes, based on a reaction-diffusion system. We also aim to understand how the scaling of polymer structure and

*Also at Material Science and Engineering Program, University of Colorado Boulder, Boulder, Colorado 80309, USA.
franck.vernerey@colorado.edu

 © 2018 American Physical Society

enzyme size and activity affect the overall degradation behavior, that we will see is suitably characterized by the speed and width of the resulting moving interface.

Falling under the category of *moving boundary problems*, these phenomena are mathematically challenging to model, often requiring numerical methods [17]. Under suitable approximations, analytical solutions do exist for infinite and semi-infinite domains. For instance, the classical example of the propagating melt-freeze interface, or Stefan problems, has been extensively studied for simple geometries in 1D [18] and isotropic spheres [19–21] with analytical solutions. In another general class of problems, Hermans [22] developed a closed-form solution for systems where the diffusing molecules (e.g., copper ions) get immobilized after reacting with another medium (e.g., cellulose xanthate), thereby propagating a sharp moving interface. An excellent review on different scenarios and strategies involving moving boundary problems in the context of diffusion can be found in the book by Crank [23]. In all the above examples, the interface is clear and sharp in separating two different phases. But, the system under investigation here often produces a fuzzy interface such that the boundary between the degraded and nondegraded regions has a finite width where both free enzymes and weak polymer cross-linking exist [24,25]. This type of interface has been modeled analytically in 1D for hydrolytic degradation of biodegradable polymers characterized by erosion rate and width that determine the nature of degradation (bulk or surface erosion) [26]. Such a simple model, however, has not been developed for enzymatic biodegradation whose chemistry and reaction kinetics vary with different enzymes [27]. In this work, we therefore present a one-dimensional centrosymmetric model of enzymatic biodegradation of solid polymers characterized by the evolving cross-linking density of the network instead of polymer water solubility.

II. MODEL AND SCALING LAWS

Let us consider an enzyme source in the shape of a sphere encapsulated in a biodegradable polymer (Fig. 1). The polymer is characterized by its cross-link density ρ and mesh size ξ, which is typically of the order of 10–100 nm. Since the sizes of enzyme molecules are in the same order of magnitude, it enables them to penetrate the mesh once released from the source. In this work, we characterize the presence of enzymes by their concentration $c(r,t)$, where r is the radial distance from the center of the source (Fig. 1). As enzymes diffuse through the polymer, they act as catalysts for polymer degradation, hence reducing the cross-link density and expanding the mesh until the so-called reverse gelation point [28] is reached. This point occurs when $\rho(r,t)=\rho_c$ and marks the sudden drop in polymer network connectivity and the transition to a fluidlike state. The critical cross-link density ρ_c is usually

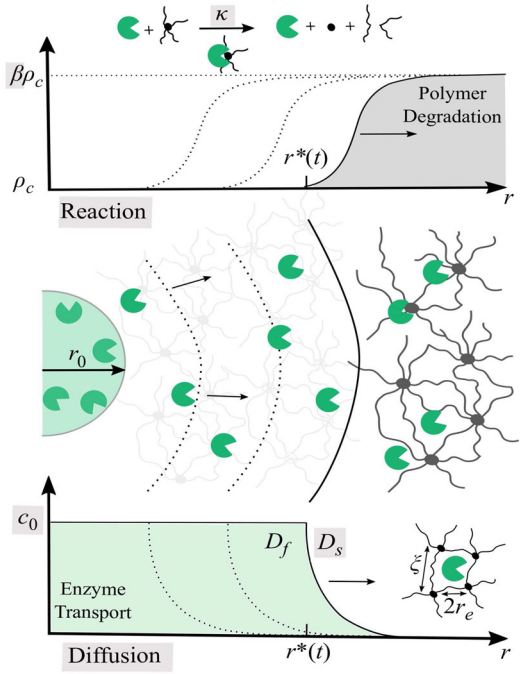

FIG. 1. Schematic illustrating the propagation of a fuzzy interface due to enzyme diffusion and degradation reaction in the biodegradable polymer. The evolution of polymer cross-link density ρ (ρ_c corresponds to reverse gelation) and enzyme concentration c are illustrated. The highlighted parameters β, κ, c_0, and D_s are the key features of the model.

identified by the ratio $1/\beta$ of minimum network connections needed for structural integrity [25,29], such that $\rho_c=\rho_0/\beta$, given an initial nondegraded cross-link density ρ_0. The coupled reaction-diffusion process can be described by Fick's law of diffusion for the enzymes and enzyme-mediated polymer degradation kinetics as

$$\frac{\partial c}{\partial t}=\frac{1}{r^2}\frac{\partial}{\partial r}\left(r^2 D\frac{\partial c}{\partial r}\right), \tag{1a}$$

$$\frac{\partial \rho}{\partial t}=-\kappa\rho c, \tag{1b}$$

where the equations are written in radial coordinates due to the problem's geometry. Here, κ is the rate constant for degradation and D denotes the enzyme diffusivity. Importantly, the diffusivity is significantly affected by degradation; before degrading, the polymer mesh resists enzyme transport such that the diffusivity D_s is given by Lustig and Peppas [30] as

$$D_s=D_f\left(1-\frac{r_e}{\xi}\right), \tag{2}$$

where r_e is the hydrodynamic radius of the enzyme molecule, ξ is the mesh size of the polymer, and D_f is the enzyme diffusivity in a fluid given by the Einstein-Stokes equation [31]. This model predicts a low diffusivity D_s when the mesh size is small compared to the enzyme r_e, and vice versa. Once

reverse gelation is reached, however, the mesh size suddenly diverges and the diffusivity becomes D_f. Based on this analysis, we assume here that the enzyme diffusivity in the degraded region ($\rho < \rho_c$) is considerably higher than in the solid polymer, i.e., $D_f \gg D_s$.

As the enzymes travel away from the source (seen here as an enzyme reservoir with concentration c_0), Eq. (1a) suggests a concentration profile that gradually decreases with distance r, as shown in Fig. 1. From the degradation kinetics in Eq. (1b), we see that this causes faster degradation closer to the source where the enzyme concentration is higher. Therefore, reverse gelation will first be reached in the immediate region around the source, at which point the polymer disintegrates into a fluid. Similar to the approach in classical Stefan problems, the spatial domain is now separated into two subdomains; one where reverse gelation has occurred [$\rho(r,t) < \rho_c$], and the other where the polymer is still intact. Given the considerably high diffusivity D_f in the first region, the enzyme concentration here saturates to that of the source, i.e., $c(r,t) = c_0$. Because of centrosymmetry, this results in a spherical interface that expands radially outward separating the fully degraded and the structurally intact polymer regions, as shown in Fig. 1. Therefore, the polymer cross-link density at the edge of this interface located at $r^*(t)$ is equal to ρ_c. Additionally, the mass of enzymes flowing across the interface should be conserved. Mathematically, these observations can be cast in terms of so-called interface conditions of the form

$$\rho|_{r^*} = \rho_c \quad \text{and} \quad -D_f \left.\frac{\partial c}{\partial r}\right|_{r^*_-} = -D_s \left.\frac{\partial c}{\partial r}\right|_{r^*_+}, \tag{3}$$

where the term $-D\partial c/\partial r$ denotes the mass flux of enzymes. Assuming no permanent deficit at the reaction site, the enzyme concentration profile is continuous across the interface, i.e., $c(r^*_+, t) = c_0$.

Since the properties in the fully degraded region ($r < r^*$) are trivial ($c = c_0, \rho < \rho_c$), we bring our attention to the solid polymer region whose inner boundary is $r = r^*(t)$, and outer boundary that is assumed sufficiently far that the enzyme flux vanishes, i.e., $-D_s \partial c/\partial r|_{r\to\infty} = 0$. Of interest in this problem is the speed $v = dr^*/dt$ at which the fluid-polymer interface travels away from the source and the extent (or width) of the degradation region from this interface. For this, we aim to solve Eq. (1) by first introducing a variable $C = cr$, changing its original form to the one-dimensional diffusion equation $\partial C/\partial t = D\partial^2 C/\partial r^2$. Now, using the transformation $R = r - r^*(t)$ to represent the solid polymer region, we anticipate and assume a traveling-wave-type solution of the form $C(R) = C_0 e^{-kR}$, where $C_0 = c_0 r^*$ should satisfy the continuity in the concentration profile and k is a parameter to be determined. Substituting for $c = C/r$ in Eq. (1) and integrating Eq. (1b) subject to interface and boundary conditions, we obtain the following solutions (see Supplemental Material [32] for more details):

$$c(R) = \begin{cases} c_0 & R \le 0 \\ c_0 r^*/re^{-kR} & R \ge 0, \end{cases} \tag{4a}$$

$$\ln(\rho/\rho_c) = \ln\beta\left(1 - \frac{1+kr^*}{1+kr}e^{-kR}\right) R \ge 0, \tag{4b}$$

where $R \ge 0$ represents the intact polymer region and $k^2 = \kappa c_0/(D_s \ln\beta)$. The value of k is obtained from the condition that at large distances ahead of the interface, the enzymes have not diffused yet, leaving the solid polymer intact with its initial cross-link density, i.e., $\rho(R\to\infty) = \beta\rho_c$. As is the case with most traveling-wave solutions, there is a transient state due to sudden initiation of interface movement when reverse gelation is first reached in the immediate region of the source. This transient state attenuates in time, and so we focus here only on the solution of the traveling wave.

Based on the above expression for k, that indeed appears extensively in Eq. (4), we identify two time scales, τ_d and τ_t, that characterize the polymer degradation and enzyme transport, respectively,

$$\tau_d = \frac{\ln\beta}{\kappa c_0} \quad \text{and} \quad \tau_t = \frac{L^2}{D_s}. \tag{5}$$

The degradation time τ_d is the time required to completely degrade the polymer when subjected to an enzyme concentration $c = c_0$. The transport time τ_t is interpreted as the time needed by the enzymes to diffuse a distance L through the solid polymer. The competition between transport and degradation is then characterized by the index

$$\gamma = \sqrt{\frac{\tau_t}{\tau_d}} = \sqrt{\frac{L^2}{D_s}\frac{\kappa c_0}{\ln\beta}}. \tag{6}$$

When $\gamma > 1$, enzyme diffusion is the rate-limiting process, and the system is reaction dominated. In contrast, when $\gamma < 1$, degradation becomes the rate-limiting process [33].

Let us now define the interface width w as the distance between the interface position [$\rho(r^*,t) = \rho_c$], and the point at which the polymer is 99% intact, i.e., $\rho(r^*+w,t) = 0.99\beta\rho_c$. The interface width provides crucial information regarding the nature of degradation ranging from surface erosion for small widths to bulk degradation for large widths. Substituting Eq. (4a) in Eq. (1a) to obtain speed and using the definition of interface width on Eq. (4b), we find that they must satisfy the equations

$$v = v_d\left(\frac{\bar{r}\gamma}{1+\bar{r}\gamma}\right), \tag{7a}$$

$$\left(1 + \frac{\bar{w}\gamma}{1+\bar{r}\gamma}\right)e^{\bar{w}\gamma} = K\ln\beta, \tag{7b}$$

where $K = -1/\ln(0.99)$, $v_d = L/\sqrt{\tau_d\tau_t}$, $\bar{r} = r^*/L$, and $\bar{w} = w/L$. As the interface moves away from the source ($\bar{r}\to\infty$), the speed and width of the interface reach their asymptotic values given by

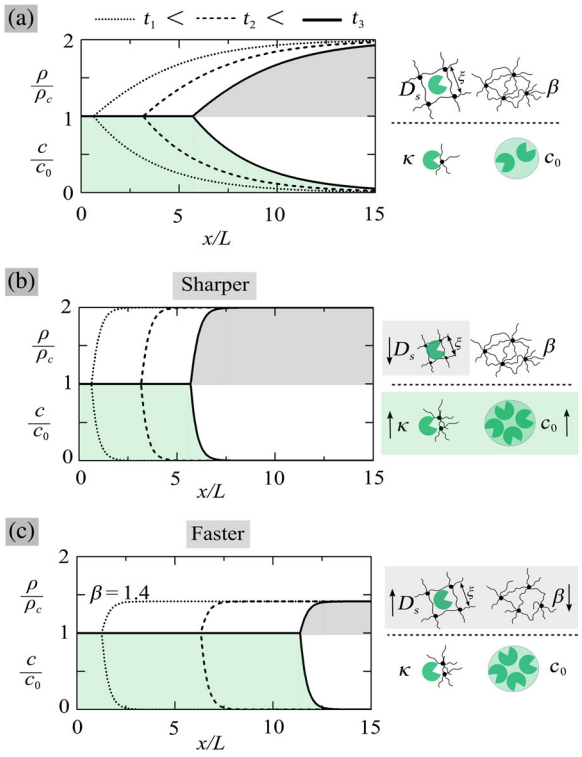

FIG. 2. Spatiotemporal degradation and enzyme profiles illustrated with (a) $\tau_t = 1$ s, $\beta = 2$, $c_0 = 1M$, and $\kappa = 0.07M^{-1}\,\mathrm{s}^{-1}$, which gives $\gamma = 0.32$; (b) sharper interface with the same speed as (a) using $\tau_t = 10$ s, $c_0 = 2M$, and $\kappa = 0.35\ \mathrm{s}^{-1}$, which gives $\gamma = 3.16$, and (c) faster interface with the same width as (b) using $\beta = 1.4$ and $\tau_t = 5$ s. The distance $x = r - r'$ is normalized to the length scale $L = r_e$, where r' is the radial distance above which the difference from the asymptotic value is negligible.

$$v = v_d = L\sqrt{\frac{D_s}{L^2}\frac{\kappa c_0}{\ln\beta}}, \tag{8a}$$

$$\bar{w} = \frac{1}{\gamma}\ln(K\ln\beta) = \sqrt{\frac{D_s}{L^2}\frac{\ln\beta}{\kappa c_0}}\ln(K\ln\beta). \tag{8b}$$

This provides important scaling relationships between interface characteristics and the four parameters β, κ, c_0, and D_s. We further note that Eqs. (8a) and (8b) describe the speed and width of a planar interface propagating in one dimension (see Supplemental Material for specific details). Equation (8b) shows that the interface width w is inversely proportional to the index γ. In other words, diffusion-dominated systems ($\gamma < 1$) are characterized by wider transitions from fluid to intact solid polymer [Fig. 2(a)]. By contrast, reaction-dominated systems ($\gamma > 1$) display sharper transitions [Fig. 2(b)]. Interestingly, Eq. (8) suggests that it is possible to carefully tune the four parameters of the model, in order to individually control the interface width and speed (Fig. 2). For instance, we show in Figs. 2(a) and 2(b) that the interface width can be controlled independently of its speed by appropriately tuning D_s, κ, and c_0. Similarly, Figs. 2(b) and 2(c) show that it is possible to control the interface speed alone by tuning D_s and β.

III. DISCUSSION

A good summary of these relationships can be obtained by plotting the interface characteristics w and v in terms of the time scales τ_t and τ_d (Fig. 3). Tuning τ_d is comparatively more flexible than τ_t, as τ_d depends on three parameters [see Eq. (5)], while τ_t is predominantly governed by the polymer mesh size ξ. Thus, using the plots in Fig. 3, one can navigate through interface design space in order to satisfy application-specific requirements. For example, in tissue engineering, spherical cartilage cells are expected to degrade the surrounding polymeric scaffold to allow the growth of new tissue [10,34]. In this scenario, it is crucial to achieve precise control of the interface characteristics as cartilage cells behave differently depending on the donor. A sharp degradation front and optimal speed are in fact the key to preserving the overall mechanical integrity of the tissue [25,35,36]. In the case of enzymatic hydrolysis of biomass, enzyme transport is restricted by a tight cellulose mesh leading to a slow surface erosion. Since fast degradation is preferable in this case [37], decreasing τ_d by increasing the enzyme source concentration c_0 or the reaction rate constant κ using different enzyme types [38] are helpful (see Fig. 3). An effective strategy to control τ_t is by mediating polymer mesh size via swelling [39,40]. This is common in hydrogels used for tissue regeneration [41,42], tissue expansion for plastic surgeries [43], and in biomass

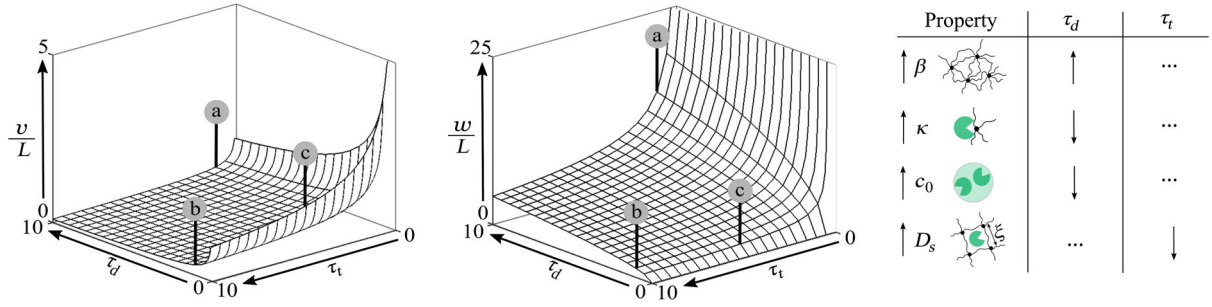

FIG. 3. Plots of interface speed v and width w, with respect to degradation time τ_d and enzyme transport time τ_t. The speed and width corresponding to Figs. 2(a)–2(c) are marked with bubbles. The trends in τ_d and τ_t due to network connectivity β, reaction rate constant κ, enzyme source concentration c_0, and enzyme diffusivity in the polymer mesh D_s, are shown.

containing cellulose [44]. The enzyme size can also be tuned to control τ_t and has been explored to achieve faster biomass degradation [45]. In addition to engineering and medical applications, natural processes involving biodegradation can also be understood based on the above scaling laws. For example, wood-rot fungi penetrate and spread by releasing a plethora of enzymes that cause a degradation of the natural polymers contained in the plant cell wall. When some host plants are more resistant (low κ) to the attack from the fungus, it responds by releasing more enzymes (higher c_0) to increase the interface speed [46,47]. Enzymatic biodegradation in the digestive tract of insects is another example where valuable insights into the physical processes are possible [48].

IV. CONCLUSION

To summarize, we have developed an analytical model of enzymatic polymer biodegradation in terms of a moving interface that propagates radially outward, characterized by its width and speed. We find the interface characteristics to depend on two competing time scales, namely, the enzyme transport and degradation times. These time scales are governed by the polymer mesh size, the enzyme source concentration, the enzymatic reaction rate constant, and the polymer network connectivity. Simple scaling laws are derived that can be used to better understand natural processes and tune the interface for engineering and biomedical applications. This will also contribute towards a more fundamental and physical understanding of enzymatic biodegradation in polymers at the microscale and provide valuable insights regarding their spatiotemporal macroscopic behavior.

F. J. V. acknowledges the support of the National Institutes of Health under Award No. 1R01AR065441 and the National Science Foundation under CAREER Award No. 1350090.

[1] P. J. Whitney, C. H. Swaffield, and A. J. Graffham, The environmental degradation of thin plastic films, Int. Biodeterior. Biodegrad. **31**, 179 (1993).
[2] R. Tsao, T. A. Anderson, and J. R. Coats, The influence of soil macroinvertebrates on primary biodegradation of starch-containing polyethylene films, J. Environ. Polym. Degrad. **1**, 301 (1993).
[3] O. Schmidt, *Wood and Tree Fungi: Biology, Protection and Use* (Springer Science & Business Media, New York, 2006).
[4] K. L. Eriksson, R. A. Blanchette, and P. Ander, *Microbial and Enzymatic Degradation of Wood and Wood Components* (Springer Science & Business Media, New York, 1990).
[5] S. Horn, G. Vaaje-Kolstad, B. Westereng, and V. G. Eijsink, Novel enzymes for the degradation of cellulose, Biotechnol. Biofuels **5**, 45 (2012).
[6] D. C. Whitcomb and M. E. Lowe, Human pancreatic digestive enzymes, Dig. Dis. Sci. **52**, 1 (2007).
[7] *Handbook of Biodegradable Polymers*, edited by Catia Bastioli, 2nd ed. (Rapra Technology, Shawbury, UK, 2016), pp. 321–368.
[8] S. Lyu and D. Untereker, Degradability of polymers for implantable biomedical devices, Int. J. Mol. Sci. **10**, 4033 (2009).
[9] J. C. Middleton and A. J. Tipton, Synthetic biodegradable polymers as orthopedic devices, Biomaterials **21**, 2335 (2000).
[10] M. P. Lutolf, J. L. Lauer-Fields, H. G. Schmoekel, A. T. Metters, F. E. Weber, G. B. Fields, and J. A. Hubbell, Synthetic matrix metalloproteinase-sensitive hydrogels for the conduction of tissue regeneration: engineering cell-invasion characteristics, Proc. Natl. Acad. Sci. U.S.A. **100**, 5413 (2003).
[11] F. J. Vernerey, A mixture approach to investigate interstitial growth in engineering scaffolds, Biomech. Model. Mechanobiol. **15**, 259 (2016).
[12] S. Lalitha Sridhar, M. C. Schneider, S. Chu, G. de Roucy, S. J. Bryant, and F. J. Vernerey, Heterogeneity is key to hydrogel-based cartilage tissue regeneration, Soft Matter **13**, 4841 (2017).
[13] E. Marshall and D. Windle, A moving boundary diffusion model in drug therapeutics, Math. Modell. **3**, 341 (1982).
[14] A. Göpferich, Mechanisms of polymer degradation and erosion, Biomaterials **17**, 103 (1996).
[15] W. C. Tan, W. Y. Wu, Z. Y. Yan, and G. B. Wen, Moving boundary problem for diffusion release of drug from a cylinder polymeric matrix, J. Appl. Math. Mech. (Engl. Transl.) **22**, 379 (2001).
[16] A. Göpferich and R. Langer, Modeling of polymer erosion, Macromolecules **26**, 4105 (1993).
[17] R. M. Furzeland, A comparative study of numerical methods for moving boundary problems, IMA J. Appl. Math. **26**, 411 (1980).
[18] J. M. Hill, *One-Dimensional Stefan Problems: An Introduction* (Longman Science & Technical, Harlow, 1987), Vol. 31.
[19] F. C. Frank, Radially symmetric phase growth controlled by diffusion, Proc. R. Soc. A **201**, 586 (1950).
[20] S. Paterson, Propagation of a boundary of fusion, Glasgow Math. J. **1**, 42 (1952).
[21] W. Scott, J. M. Classical, B. S. W. Mccue, B. Wu, J. M. Hill, S. W. McCue, B. Wu, and J. M. Hill, Classical two-phase Stefan problem for spheres, Proc. R. Soc. A **464**, 2055 (2008).
[22] J. Hermans, Diffusion with discontinuous boundary (1), J. Colloid Sci. **2**, 387 (1947).
[23] J. Crank, *The Mathematics of Diffusion* (Oxford University Press, Oxford, 1979).
[24] V. Dhote and F. J. Vernerey, Mathematical model of the role of degradation on matrix development in hydrogel scaffold, Biomech. Model. Mechanobiol. **13**, 167 (2014).
[25] U. Akalp, S. J. Bryant, and F. J. Vernerey, Tuning tissue growth with scaffold degradation in enzyme-sensitive hydrogels: a mathematical model, Soft Matter **12**, 7505 (2016).
[26] S. Lyu, R. Sparer, and D. Untereker, Analytical solutions to mathematical models of the surface and bulk erosion of solid polymers, J. Polym. Sci. B **43**, 383 (2005).
[27] A. Banerjee, K. Chatterjee, and G. Madras, Enzymatic degradation of polymers: a brief review, Mater. Sci. Technol. **30**, 567 (2014).

[28] D. R. Miller and C. W. Macosko, A new derivation of post gel properties of network polymers, Rubber Chem. Technol. **49**, 1219 (1976).
[29] P. J. Flory, *Principles of Polymer Chemistry* (Cornell University Press, Ithaca, 1953).
[30] S. R. Lustig and N. A. Peppas, Solute diffusion in swollen membranes .9. scaling laws for solute diffusion in gels, J. Appl. Polym. Sci. **36**, 735 (1988).
[31] C. L. Bell and N. A. Peppas, Biomedical membranes from hydrogels and interpolymer complexes, in *Biopolymers II* (Springer, Berlin, Heidelberg, 1995), Vol. 122, pp. 125–175.
[32] See Supplemental Material at http://link.aps.org/supplemental/10.1103/PhysRevApplied.9.031001 for the detailed derivation.
[33] F. V. Burkersroda, L. Schedl, and A. Göpferich, Why degradable polymers undergo surface erosion or bulk erosion, Biomaterials **23**, 4221 (2002).
[34] F. J. Vernerey, E. C. Greenwald, and S. J. Bryant, Triphasic mixture model of cell-mediated enzymatic degradation of hydrogels, Comput. Methods Biomech. Biomed. Eng. **15**, 1197 (2012).
[35] V. Dhote, S. Skaalure, U. Akalp, J. Roberts, S. J. Bryant, and F. J. Vernerey, On the role of hydrogel structure and degradation in controlling the transport of cell-secreted matrix molecules for engineered cartilage, J. Mech. Behav. Biomed. Mater. **19**, 61 (2013).
[36] S. Chu, S. L. Sridhar, S. C. Skaalure, F. J. Vernerey, and S. J. Bryant, Understanding the spatiotemporal degradation behavior of aggrecanase-sensitive Poly(ethylene glycol) hydrogels for use in cartilage tissue engineering, Tissue Eng. Part A **23**, 795 (2017).
[37] B. Yang, Z. Dai, S.-Y. Ding, and C. E. Wyman, Enzymatic hydrolysis of cellulosic biomass, Biofuels **2**, 421 (2011).
[38] L. R. Lynd, Overview and evaluation of fuel ethanol from cellulosic biomass: technology, economics, the environment, and policy, Annu. Rev. Energy Environ. **21**, 403 (1996).
[39] G. I. Mantanis, R. A. Young, and R. M. Rowell, Swelling of compressed cellulose fiber webs in organic liquids, Cellulose **2**, 1 (1995).
[40] U. Akalp, S. Chu, S. C. Skaalure, S. J. Bryant, A. Doostan, and F. J. Vernerey, Determination of the polymer-solvent interaction parameter for PEG hydrogels in water: Application of a self learning algorithm, Polymer **66**, 135 (2015).
[41] G. D. Nicodemus and S. J. Bryant, Cell encapsulation in biodegradable hydrogels for tissue engineering applications, Tissue Eng. Part B **14**, 149 (2008).
[42] S. J. Bryant and F. J. Vernerey, Programmable hydrogels for cell encapsulation and neo-tissue growth to enable personalized tissue engineering, Adv. Healthcare Mater. **7**, 1700605 (2017).
[43] A. Lendlein and A. Sisson, *Handbook of Biodegradable Polymers: Isolation, Synthesis, Characterization and Applications*, edited by A. Lendlein and A. Sisson (Wiley-VCH Verlag GmbH & Co. KGaA, Weinheim, Germany, 2011).
[44] K. W. Lin, M. R. Ladisch, M. Voloch, J. A. Patterson, and C. H. Noller, Effect of pretreatments and fermentation on pore size in cellulosic materials, Biotechnol. Bioeng. **27**, 1427 (1985).
[45] R. K. Dasari and R. Eric Berson, The effect of particle size on hydrolysis reaction rates and rheological properties in cellulosic slurries, Applied biochemistry and biotechnology **137–140**, 289 (2007).
[46] E. T. Reese, Degradation of polymeric carbohydrates by microbial enzymes, in *The Structure, Biosynthesis and Degradation of Wood* (Springer, Boston, 1977), pp. 311–367.
[47] Á. T. Martínez, M. Speranza, F. J. Ruiz-Dueñas, P. Ferreira, S. Camarero, F. Guillén, M. J. Martínez, A. Gutiérrez, and J. C. Del Río, Biodegradation of lignocellulosics: Microbial, chemical, and enzymatic aspects of the fungal attack of lignin, Int. Microbiol. **8**, 195 (2005).
[48] W. R. Terra, C. Ferreira, B. P. Jordao, and R. J. Dillon, Digestive enzymes, in *Biology of the Insect Gut* (Springer, Dordrecht, 1996), pp. 153–194.